Hindawi
International Journal of Polymer Science
Volume 2018, Article ID 4960416, 8 pages
https://doi.org/10.1155/2018/4960416

Research Article

Synthesis and Characterization of O-Acetyl-chitosan Acetic Ester

Fangfang Cheng,[1,2] Bingbing Wang,[2] and Yanzhi Xia[1,2]

[1]*Collaborative Innovation Center for Marine Biomass Fibers, Materials and Textiles of Shandong Province, Institute of Marine Biobased Materials, Qingdao University, 308 Ningxia Road, Qingdao 266003, China*
[2]*College of Materials Science and Engineering, Qingdao University, 308 Ningxia Road, Qingdao 266003, China*

Correspondence should be addressed to Yanzhi Xia; qdxyzh@163.com

Received 13 April 2018; Revised 4 September 2018; Accepted 29 September 2018; Published 9 December 2018

Academic Editor: Cornelia Vasile

A novel amphipathic chitosan derivative, O-acetyl-chitosan acetic ester (ACHA), was synthesized by the reaction of chitosan with acetic acid in the presence of thionyl chloride. The physicochemical properties of ACHA were characterized by FTIR, ^{1}H NMR, TGA, and XRD. The yield (Y) of ACHA was 79.4%, and the degree of acetylation (DA) of ACHA was 1.04. Compared to CS, ACHA could be dissolved in many organic solvents, deionized water, and aqueous solution. Our results showed that ACHA exhibited a superior antibacterial activity against *Escherichia coli*, *Pseudomonas aeruginosa*, and *Staphylococcus aureus*. These findings indicated that ACHA was preferable for use as antimicrobial agents in wound healing, food preservative, and tissue engineering.

1. Introduction

Nowadays, antibacterial agents derived from natural substance have attracted enormous attention, due to their excellent antibacterial efficiency and favorable biocompatibility [1]. In addition to their own structural characteristics, the stability and durability of natural antibacterial agents are primary factors restricting their wide applications [2, 3]. Chitosan (CS), the second most abundant natural biopolymer, is derived from the chitin of crustacean or mushroom shells. As a representative natural antibacterial agent, CS has been widely used in the field of packaging, medical applications, pharmaceutics, biomedicine, biotechnology, and textiles [4, 5]. CS possesses a wide spectrum of activity [6–8] and a high killing rate against various bacteria, filamentous fungi, and yeasts [9–11], which makes it as an ideal pretreatment material applied in textile dyeing, textile printing, textile processing, wool dyeing, and shrink proofing [12–15]. However, its linear, rigid, and semicrystalline structure makes CS insoluble in aqueous solutions above pH ~ 6.5 (pK_a ~ 6.3) and organic solvents. The poor solubility of CS is considered as the major obstacle limiting its potential applications. Therefore, how to improve the solubility of CS while retaining its antibacterial activity is still the key problem needed to be resolved [16].

To date, chemical modifications which are aimed at enhancing the solubility of CS, such as carboxymethylation and quaternisation, usually compromise the antibacterial activity and/or the safety of CS. For instance, carboxymethylated chitosan gained a much better water solubility, whereas its antibacterial activity as found to be reduced. Quaternisation modification increased both the solubility and antibacterial activity of CS; however, it also introduced potential cytotoxicity to the modified chitosan. Therefore, to improve water solubility, the antibacterial activity and biocompatibility simultaneously are key issues to be figured out for the chitosan-based natural antibacterial material [17]. Acylation of CS was found to be able to effectively improve the performance of antibacterial materials. In order to obtain the chitosan derivatives, researchers chemically functionalized CS through its hydroxyl groups. For example, the esterification of CS through the hydroxyl at C-6 position has been well studied and esterified CS exhibited several superior biological properties, such as nontoxicity, good solubility, and biocompatibility. Till now, there are two main methods to synthesize chitosan ester. One method is to synthesize chitosan ester

from acid and CS with a powerful dehydrating agent as a catalyst at high temperature. The other one is to protect the amino group first, since it is more reactive than the other groups. Then, the amino-protecting group is removed after the esterification. Both of the two methods have advantages and disadvantages. The former one is easier, but the degree of substitution is usually very low. The latter one is more complex and difficult. Therefore, the esterification that can be conducted at room temperature with simplified experimental steps is still in urgent demand.

In this study, a novel chitosan derivative, *O*-acetyl-chitosan acetic ester (ACHA), was directly obtained by esterification of CS with acetic acid in the presence of sulfur dichloride at room temperature. This simple method requires benign reaction conditions and less reaction time. The chemical structure and physical properties of ACHA were characterized by FTIR, TGA, ^{1}H NMR, and XRD techniques. We have carefully studied its solubility in water, 1% acetic acid aqueous solution, and organic solvents at $25 \pm 0.5^\circ$C as well as its antibacterial activities against *Escherichia coli* (*E. coli*), *Staphylococcus aureus* (*S. aureus*), and *Pseudomonas aeruginosa* (*P. aeruginosa*).

2. Experimental

2.1. Materials. CS (food-grade) was purchased from Huipu Biotechnology Co. Ltd. (Xi'an, China) and used as received without further purification. The molecular weight (MW) of CS was 400 kDa, and the degree of deacetylation (DD) was 90.5% [18]. Acetic acid, thionyl chloride, and all the other reagents (AR) used in the study were purchased from Haihui Chemical Reagent Company (Qingdao, China) with the analytical reagent grade. *S. aureus*, *E. coli*, and *P. aeruginosa* used for the antibacterial activity test were supplied by Microbiology Laboratory of College of Marine Life Science.

2.2. Synthesis of ACHA. ACHA was prepared by the reaction of CS with acetic acid in the presence of thionyl chloride. Briefly, 7 g of CS (40 mmol calculated as glucosamine units) was mixed thoroughly with 35 mL of pure acetic acid and sonicated at room temperature (53 kHz, 260 W) for 30 min. Then, 8.85 mL of thionyl chloride was slowly added into the above mixture by a dropping funnel under stirring at 25°C for 90 min, followed by precipitation in alcohol. The reaction mixture was filtered, dissolved in distilled water, dialyzed, concentrated, and spray-dried. Finally, the expected ACHA was obtained and stored in a vacuum dried at room temperature for further use.

The yield (Y) was gravimetrically determined by applying the following equations [19].

$$W_2 = \frac{W_1 \times 250}{166}, \qquad Y(\%) = \frac{W_3}{W_2} \times 100\%, \tag{1}$$

where W_1 (g) is sample weight, W_2 (g) is the theoretical weight, and W_3 (g) is the weight of the reaction product. 166 is the molecular weight of the chitosan monomer, and 250 is the molecular weight of the complete acylation reaction chitosan monomer.

2.3. Characterizations

2.3.1. FTIR and ^{1}H NMR Spectroscopy. Fourier transform infrared spectroscopy (FTIR) was used to examine the peak variations of the hydroxyl groups and the amine groups before and after reaction (NEXUS-870, Nicolet Instrument Co., USA). About 2 mg of the sample was fully ground and mixed with 110 mg of KBr. All spectra were scanned against a blank KBr pellet background in the range of 4000–400 cm^{-1} with 2.0 cm^{-1} resolution. The FTIR spectra were normalized, and the major vibration bands were assigned to the main chemical groups.

The ^{1}H NMR spectra were obtained on a clear magnetic resonance spectrometer (AV400, Bruker, Germany). CS was dissolved in mixed solvents of DCl and D_2O, and ACHA was dissolved in D_2O. The degree of acetylation (DA) of ACHA was calculated from the peak areas in NMR spectra by an integral method.

2.3.2. Thermogravimetric Analysis (TGA). TGA of the samples was characterized by a Rubotherm DynTHERM thermogravimetric analyzer (Rubotherm Corp., Germany). Samples were heated from 50 to 500°C at a constant heating rate of 10°C/min under N_2 protection (20 mL/min) during the analysis.

2.3.3. X-Ray Diffraction (XRD). XRD patterns of the samples were recorded on a D-8 advance diffractometer (Bruker AXS, Germany) with a Cu Kα radiation ($\lambda = 0.154$ nm), operating at 40 kV and 40 mA. The diffraction data was collected at 2θ values from 5° to 60°, and the scanning rate was 4°/min.

2.4. Solubility Test. The solubility of the samples was assessed by applying methods of Ma et al. [20]. The finely powdered samples (100 mg) were accurately weighed in a stoppered tube (16 mm in internal diameter and 160 mm long) and mixed with 0.1 mL of certain solvent, followed by treatment under high-intensity ultrasound (53 kHz, 260 W) for 3 h at $25 \pm 0.5^\circ$C to afford a completely dissolved clear solution. The transparency of the solution was observed by UV-visible spectroscopy. Solubility was expressed as amount (mg) of the test sample dissolved in 1 mL of solvent.

The dissolution rates in distilled water and 1% acetic acid aqueous solution were studied in order to develop a comprehensive understanding of samples. The dissolution rates of CS and ACHA (500 mg) were detected, respectively, by dissolving the materials in distilled water and 1% (*w*/*v*, 50 mL) acetic acid aqueous solution with stirring under room temperature. The mixtures were stirred until a stable and clear solution was formed. Solubility test was performed in triplicate, and the results were processed using a statistical method.

2.5. Antimicrobial Test. The antimicrobial activity was investigated using *E. coli*, *P. aeruginosa* (G–), and *S. aureus* (G+) as test microorganisms. *E. coli* and *S. aureus* were the representative strains in the nature used for the antibacterial susceptibility test, while *P. aeruginosa* was a common

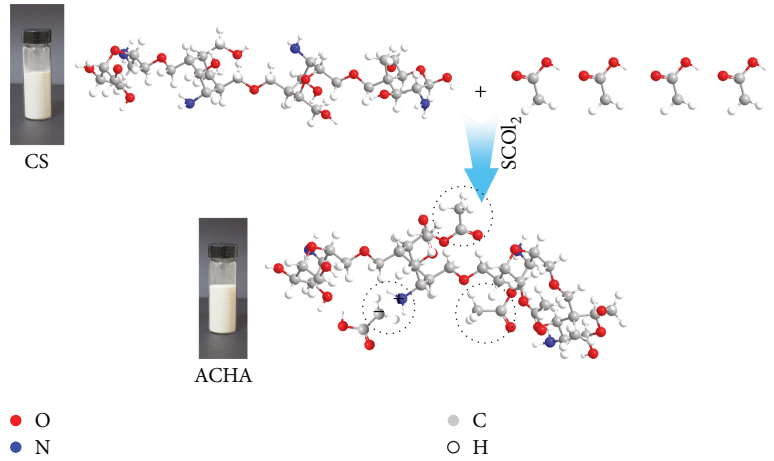

Figure 1: The photos, chemical structure of CS and ACHA, and the schematic illustration of the synthesis of O-acetyl-chitosan acetic ester (ACHA).

bacterium which could cause wound infection. A representative microbe colony was picked off with an inoculating needle, placed in 25 mL sterile nutrient broth, and then incubated in a shaker at a speed of 100 rpm at 37°C for 24 h. The bacterial suspension was then diluted with sterile physiological saline to 10^3–10^4 CFU/mL and used for the antibacterial test [21, 22].

The inhibition rates of CS and ACHA against *E. coli*, *S. aureus*, and *P. aeruginosa* were determined through the use of agar plates [1]. The main solution of CS and ACHA was prepared by dissolving the materials in 1% (*w*/*v*) acetic acid aqueous solution, respectively. The mixtures were stirred until a stable and clear solution was formed. The processed filter papers which were immersing in the above solution were put on agar plates covered with bacteria, and all the plates were incubated at 37°C for 24 h. The CS, ACHA, and acetic acid solutions with different concentrations were prepared by duplicate twofold serial dilutions and then sterilized by a 0.22 μm filter. The methods for preparing nutrient agar plates are described as follows: a homogeneous mixture of nutrient agar was prepared and sterilized by autoclaving at 121°C for 25 min. The sterilized solution (about 25 mL) was poured into sterile Petri dishes to form a solidified nutrient agar plate in a bacteria-free operating environment, followed by the addition of 100 μL of bacterial suspension and then 100 μL of the samples with different concentrations was also added. Both of them were spread uniformly by a sterilized SS-spreader. In addition, the samples in the control group were replaced by sterile water. All the samples were plated in triplicate on agar plates, and all the plates were incubated at 37°C for 24 h. Then, the plates were taken out to count the colonies. The inhibition rate (IR) was calculated according to (2), and the IR data were treated by a statistical method.

$$\mathrm{IR}(\%) = \frac{N_1 - N_2}{N_1} \times 100, \quad (2)$$

where N_1 is the number of colony on the plates with sterile water and N_2 is the number of colony after treating with the test materials and acetic acid aqueous solutions at different concentrations.

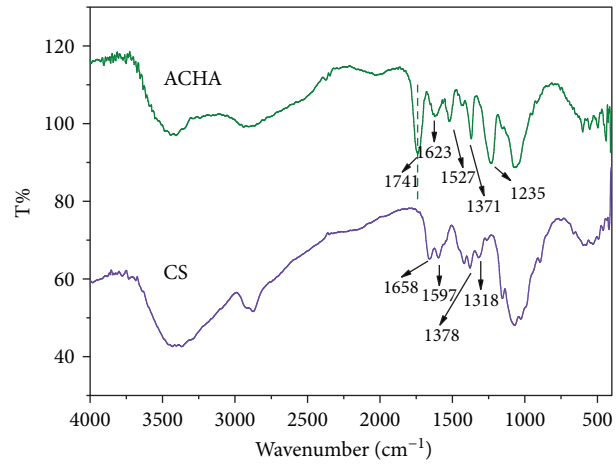

Figure 2: FTIR spectra of chitosan (CS) and O-acetyl-chitosan acetic ester (ACHA).

3. Results and Discussion

3.1. Characterizations. The photos and chemical structure of CS and ACHA are shown in Figure 1. Different from the white CS, ACHA showed canary yellow. The synthesis procedure of ACHA is shown in Figure 1. The yield (Y) of ACHA was calculated to be 79.4%.

In the FTIR spectrum of CS, the strong broad band at around 3200–3600 cm^{-1} should be attributed to stretching vibration of -OH and inter- and extramolecular hydrogen bonding of chitosan molecules (Figure 2). The characteristic peaks at 1658, 1597, 1318, 1072, and 1026 cm^{-1} should correspond to the amide I, amine II, and amide III absorption bands of CS and C-O stretching vibration in C_3-OH and C_6-OH, respectively. In comparison with CS, the absorption bands of ACHA moved from 1597 cm^{-1} (amide II) to 1527 cm^{-1}, evidencing the formation of -C-N- and NH functionalities. The appearance of a band at 1623 cm^{-1} can be

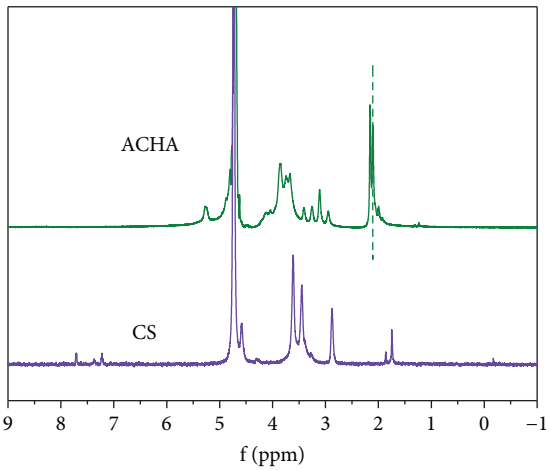

FIGURE 3: The ^{1}H NMR spectra of chitosan (CS) and O-acetyl-chitosan acetic ester (ACHA).

assigned to the stretching vibration of -NH_3^+, which indicated that -NH_2 groups were still retained on the backbone of ACHA. The characteristic absorption bands of ACHA at 1371 cm^{-1} should correspond to the stretching vibration of -CH_3. Besides, the new absorption peak at 1741 and 1235 cm^{-1} in the FTIR spectrum of ACHA should be attributed to the characteristic peak of saturated fatty acid ester groups (-CO-O-). The characteristic peaks at 1072 and 1026 cm^{-1} became weak, which suggested that the esterification reaction occurred between acetic acid and -OH of CS. These results demonstrated that ACHA had been successfully synthesized.

The ^{1}H NMR spectra of CS and ACHA are shown in Figure 3. For the ^{1}H NMR spectrum of CS, the peak at 1.93 ppm can be assigned to the three protons of *N*-acetyl glucosamine and the peak at 3.18 ppm should correspond to the proton of glucosamine residues (H-2). The peaks from 3.25 to 4.00 ppm should be attributed to the nonanomeric protons (H-3, 4, 5, and 6), while a small peak at 4.66 ppm represents anomeric proton (H-1) of glucosamine residues and *N*-acetyl glucosamine, respectively. Compared with CS, the ^{1}H NMR spectrum of ACHA had a great difference. In the ^{1}H NMR spectrum of ACHA, the peaks from 3.25 to 4.00 ppm were reduced and signal at 1.93 ppm became stronger due to the presence of more acetyl hydrogen. The results indicated that ACHA was comprised of the ammonium group, the acetyl group, and the other framework. This result was consistent with those from the FTIR analysis.

The degree of acetylation (DA) of ACHA was defined as the number of the acetyl group linked to -OH per sugar residue of CS. It was calculated by an integral method of peak areas in the ^{1}H NMR spectrum of ACHA according to the following equation.

$$\mathrm{DA} = \frac{[\mathrm{CH_3}]}{3H_1} - (1 - \mathrm{DD}), \tag{3}$$

where H_1 is the integral of anomeric proton of CS (δ = 4.66 ppm), $[CH_3]$ is the integral of the acetyl hydrogen (δ = 1.93 ppm), and DD is the degree of deacetylation of CS (90.5%). By the calculation, the result of DA for ACHA was 1.04.

The thermal stability of CS and ACHA was studied by TGA (Figure 4(a)). Both CS and ACHA had two stages of weight loss, and the small weight loss at 100°C should correspond to the removal of volatile products and free water. Further thermal degradation not only resulted in dehydration and fragmentation of the saccharide rings but also led to depolymerization and decomposition of the side chain. For CS, the first stage at about 100°C exhibited 0.97% weight loss and a further maximum weight loss of 58.88% started at about 172°C (Figure 4(a)). CS exhibited a high speed of decomposition between 271.92 and 330°C, reaching the maximum at 307.49°C with the peak width of 37.95°C (Figure 4(a)). ACHA also showed two stages of weight loss as shown in Figure 4(a). The first stage started at about 100°C revealed about 2.93% weight loss. The second stage started at about 150°C revealed about 66.47% weight loss. The high speed of decomposition existed between 198.91 and 230°C, reaching the maximum at 211.06°C with the peak width of 24.57°C. The results above showed that CS had better thermal stability than ACHA. In Figure 4(b), the second stage of decomposition of CS and ACHA exhibited some differences. ACHA had a lower decomposition speed compared with CS. This phenomenon should be attributed to the lower decomposition temperature of ester and ionic bonds in ACHA than hydroxyl and amino groups in CS. The maximal temperature and peak width of ACHA became narrower which should be attributed to the different molecular structures, in which the new groups were introduced leading to the breakage of the hydrogen bond within CS. Furthermore, it was estimated that increasing the number of side chains might lower the decomposition temperature [20, 23].

X-ray diffraction was used to study the crystalline properties of CS and ACHA. As shown in Figure 5, the diffractogram of CS consisted of two major crystalline peaks located at around 10.8° and 20.2°. Compared with CS, the XRD of ACHA exhibited some changes in their diffraction angles, peak intensity, and peak width. For ACHA, the peak at 10.8° and 20.2° disappeared and a new peak at 24.7° was observed with increased intensity and width. It is well known that peak intensity and width in the XRD pattern are bound up with crystallite size [24]. The weaker and broader peak implied that there was more amorphous phase in the ACHA matrix and the crystallinity of ACHA was lower than that of CS. These results might be attributed to the combined effects of molecular interaction, symmetry, and stereoregularity. It is worth noting that the new introduced groups should link to CS backbones and its amino group by covalent binding and ionic bond, respectively. Besides, the new introduced groups might lead to the changes of symmetry and stereoregularity of CS. Therefore, their different crystallinities would inevitably induce different properties.

3.2. Solubility Test. To evaluate the stability and solubility of the samples, CS and ACHA were dissolved in different solvents, respectively. As shown in Table 1, the results showed that CS did not dissolve in normal solvents except

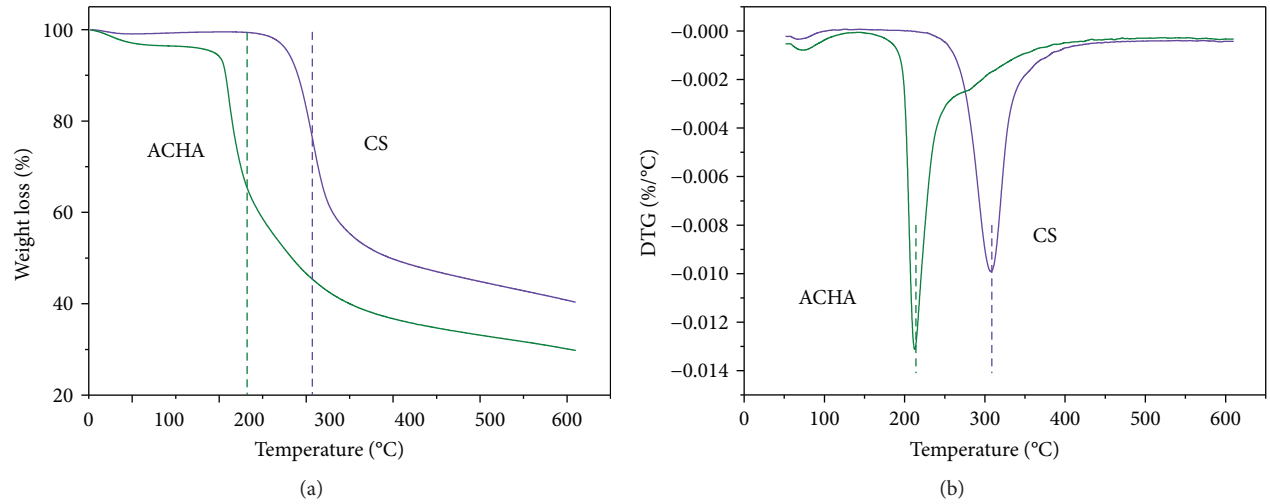

Figure 4: (a) TGA and (b) DTG thermograms of chitosan (CS) and O-acetyl-chitosan acetic ester (ACHA).

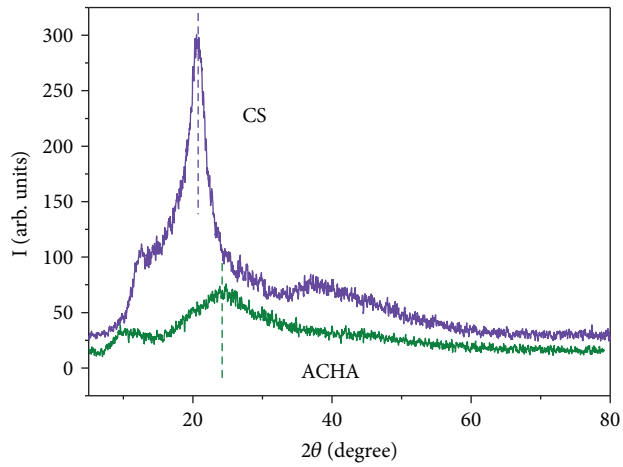

Figure 5: XRD of chitosan (CS) and O-acetyl-chitosan acetic ester (ACHA).

Table 1: Solubility of chitosan (CS) and O-acetyl-chitosan acetic ester (ACHA) in different solvents at 25 ± 0.5°C.[a]

Sample Solvent	CS Solubility (mg/mL)	ACHA Solubility (mg/mL)
Normal saline, 0.9% (*w*/*v*)	—	227 ± 4.23
Benzalkonium bromide	—	121 ± 2.82
Ethanediol	—	25.71 ± 0.82
Isopropyl alcohol	—	15.15 ± 0.76
Deionized water	—	240 ± 5.33
Acetic acid, 1% (*w*/*v*)	102 ± 2.2	220 ± 3.19
Sodium hydroxide, 1% (*w*/*v*)	—	—

[a]Values represent mean ± S.D., $n = 3$. "—" means insoluble.

1% (*w*/*v*) acetic acid aqueous solution. When CS was dissolved in acetic acid aqueous solution, the dissolution time was more than half an hour (Figure 6). On the other hand, ACHA exhibited good solubility in deionized water (240 ± 5.33 mg/mL), 1% (*w*/*v*) acetic acid aqueous solution (220 ± 3.19 mg/mL) (Table 1), and 0.9% (*w*/*v*) normal saline (227 ± 4.23 mg/mL). Moreover, ACHA can also be dissolved in organic solvents such as ethanediol and isopropyl alcohol. ACHA exhibited a slightly higher solubility in deionized water than in other media, probably because the increased ionic strength led to the decreased solubility of ACHA. The introduction of acetyl groups into CS molecular skeleton effectively weakened the strong intra- and intermolecular hydrogen bonding interaction within esterified chitosan. The variation of crystallinity and interaction of chitosan resulted in the water solubility of its derivatives accordingly. Furthermore, the hydrophobic acetyl groups grafted onto CS through the 3,6′-OH hydrophilic groups affected the water solubility of chitosan making it amphipathic. When ACHA was dissolved in distilled water (Figure 6(a)) and 1% acetic acid aqueous solution (Figure 6(b)), the dissolution time was only 6 minutes. All in all, there were large differences in the dissolution rate between CS and ACHA solutions in distilled water and 1% acetic acid aqueous solution.

3.3. Antibacterial Assays. Antibacterial capacities of CS and ACHA against *E. coli* and *P. aeruginosa* (Gram-negative bacteria) and *S. aureus* (Gram-positive bacteria) were evaluated at different concentrations for 24 h (Figure 7 and Tables 2–4). When the concentrations of CS and ACHA were both 1%, the inhibition zone test indicated that ACHA had more obvious inhibiting effects than CS on *E. coli*, *P. aeruginosa*, and *S. aureus*. And the antibacterial rates of ACHA towards *E. coli* and *P. aeruginosa* were both over 90%, while the inhibition rates of CS were, respectively, 83% and 88%, demonstrating that ACHA had satisfactory antibacterial activity compared with CS. So far, the specific antibacterial mechanism of CS [25, 26] and its derivatives still remains unclear. The most acceptable mechanism was mediated by the electrostatic forces between the protonated amino groups ($-NH_3^+$) of CS and the electronegative charges on microbial cell surface and the inside of microbial cells.

This electrostatic interaction might have the following two influences: (i) the external influence by promoting

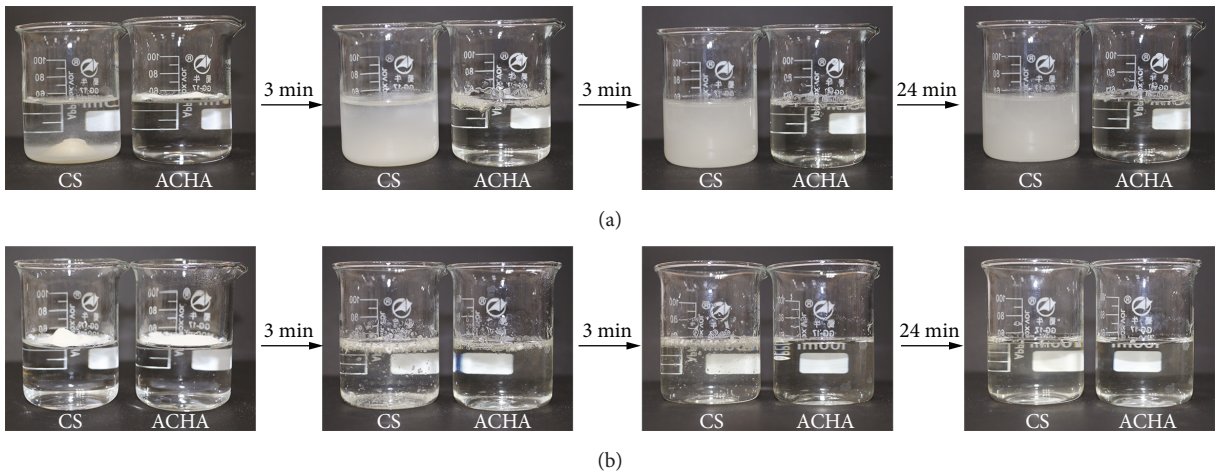

Figure 6: The dissolution rates of chitosan (CS) and O-acetyl-chitosan acetic ester (ACHA) in distilled water (a) and 1% acetic acid aqueous solution (b).

Figure 7: The inhibition zones of chitosan (CS) and O-acetyl-chitosan acetic ester (ACHA) in 1% acetic acid aqueous solution. (a) Pseudomonas aeruginosa; (b) Escherichia coli; (c) Staphylococcus aureus. (1) The filter paper immersed in 1% (*w*/*v*) acetic acid aqueous solution. (2) The filter paper immersed in 1% (*w*/*v*) ACHA aqueous solution (obtained from dissolving 1 g ACHA in 100 mL 1% acetic acid aqueous solution). (3) The filter paper immersed in 1% (*w*/*v*) CS aqueous solution (obtained from dissolving 1 g CS in 100 mL 1% acetic acid aqueous solution).

Table 2: Inhibition rate of chitosan (CS) and O-acetyl-chitosan acetic ester (ACHA) on *E. coli*.[a]

Sample concentration (%) (*w*/*v*)	0.03125	0.0625	0.125	0.25	0.5	1
	Inhibition rate (%)					
Acetic acid	2.7 ± 0.9	7.1 ± 1.2	14.1 ± 1.0	16.0 ± 1.1	19.8 ± 1.2	24.6 ± 2.7
CS	20.7 ± 2.2	47.5 ± 3.1	54.8 ± 2.3	62.1 ± 2.0	74.1 ± 0.9	83.2 ± 1.2
ACHA	27.1 ± 1.9	53.6 ± 2.2	62.3 ± 2.6	69.3 ± 2.4	81.3 ± 0.9	93.7 ± 0.7

[a]Values represent mean ± S.D., $n = 3$. *E. coli*: *Escherichia coli*.

Table 3: Inhibition rate of chitosan (CS) and O-acetyl-chitosan acetic ester (ACHA) on *S. aureus*.[a]

Sample concentration (%) (*w*/*v*)	0.03125	0.0625	0.125	0.25	0.5	1
	Inhibition rate (%)					
Acetic acid	2.2 ± 1.9	9.1 ± 2.7	16.3 ± 3.3	19.8 ± 1.4	22.3 ± 2.9	27.2 ± 2.1
CS	63.9 ± 2.1	70.2 ± 1.3	90.8 ± 1.7	93.4 ± 1.3	95.7 ± 0.2	100 ± 0.0
ACHA	75.1 ± 2.1	83.6 ± 1.2	95.2 ± 0.3	97.0 ± 0.3	99.0 ± 0.3	100 ± 0.0

[a]Values represent mean ± S.D., $n = 3$. *S. aureus*: *Staphylococcus aureus*.

changes of permeation property of the microbial cell membrane hydrolysis of the peptidoglycans in the microbial cell envelope, leading to the leakage of proteinaceous and other intracellular constituents and (ii) the internal influence by CS penetrating into the cells and combining with microbial DNA or negatively charged cytoplasm, leading to distinct

Table 4: Inhibition rate of chitosan (CS) and O-acetyl-chitosan acetic ester (ACHA) on *P. aeruginosa*.[a]

Sample concentration (%) (*w*/*v*)	0.03125	0.0625	0.125	0.25	0.5	1
			Inhibition rate (%)			
Acetic acid	2.5 ± 1.3	8.1 ± 1.2	14.3 ± 1.2	16.2 ± 1.4	18.8 ± 1.1	23.6 ± 1.7
CS	20.6 ± 1.9	48.3 ± 2.1	55.8 ± 1.3	63.1 ± 1.7	76.1 ± 1.1	88.2 ± 1.2
ACHA	24.1 ± 1.6	52.6 ± 1.2	64.3 ± 2.1	73.3 ± 1.4	81.3 ± 1.2	94.7 ± 1.1

[a]Values represent mean ± S.D., $n = 3$. *P. aeruginosa*: *Pseudomonas aeruginosa*.

physiological derangements [27]. ACHA exerted the higher antibacterial activity than CS which might be due to the introduction of a large number of acetyl groups as the hydrophobic group into the chitosan backbone to endow ACHA with amphiphilicity. Meanwhile, the introduction of acetyl into the CS molecular skeleton resulted in effectively weaken inter- and extramolecular hydrogen bonding of CS molecules. Furthermore, the formation of the ester bond allowed ACHA to possess the higher hydrophobicity leading to the easier interaction with bacterial cells than chitosan. Therefore, ACHA could be more prone to enter into microorganisms and impair the structure and function of the microorganisms by destroying the cell walls and inhibiting the DNA transcription. Sun et al. [24], Sajomsang et al. [28], and Yang et al. [29] demonstrated that hydrophobic characteristic of CS was prone to the interaction between CS and bacterial cells. ACHA had higher hydrophobicity and was more prone to interact with bacterial cells than CS. This could explain why the antibacterial activity of ACHA was higher than the parent CS. Besides, CS and ACHA were more active against the Gram-positive bacteria than against the Gram-negative bacteria. This result was similar to that from Sajomsang et al. [30]. When the concentrations of CS and ACHA were both 0.25%, the inhibition rates against *S. aureus* were 93.4 and 97%, respectively; meanwhile, the corresponding inhibition rates against *E. coli* were 62.1 and 69.3% and those against *P. aeruginosa* were 63.1 and 73.3%, respectively. This might be attributed to the different structures of bacterial cell wall. The cell wall of Gram-positive bacteria is mainly composed of a porous network of peptidoglycan, crosslinking relatively loose, which makes the CS and ACHA access to the cell easily. However, the structure of the cell wall of Gram-negative bacteria is very complex, as there is an outer membrane constituted of lipopolysaccharide, lipoprotein, and phospholipids besides a thin peptidoglycan layer. The outer membrane can regulate and control the entrance of outside elements, which forms a potential barrier against the foreign molecules with high molecular weight. Therefore, CS and its derivative have different effects on the two kinds of bacteria.

4. Conclusions

O-Acetyl-chitosan acetic ester (ACHA), an amphiphilic chitosan derivative, was synthesized by using chitosan (CS) and acetic acid under the catalysis of sulfur dichloride, with the yield of 79.4%. FTIR and ^{1}H NMR spectra confirmed that the acetyl groups were selectively attached to the amino and hydroxyl groups of chitosan. The DA of ACHA was calculated to be 1.04. TGA and DTG studies revealed that ACHA and CS had similar thermal stabilities, while the decomposition speed of ACHA was lower than that of CS. XRD studies implied that acylation reaction might lead to the destruction of crystalline structure of CS, since there was more amorphous phase in the ACHA matrix than that in CS. ACHA exhibited much better solubility than CS in both distilled water and 1% (*w*/*v*) acetic acid aqueous solution, which was mainly related to the amphipathicity of ACHA. Additionally, ACHA not only exhibited higher antimicrobial activity than CS against *E. coli*, *P. aeruginosa*, and *S. aureus* but also expanded the pH spectrum of CS in different environments. All these results suggested that ACHA had potential to be applied as antimicrobial agents in wound healing, food preservative, and tissue engineering.

Data Availability

The data used to support the findings of this study are included within the article.

Conflicts of Interest

The authors declare that they have no conflicts of interest.

Acknowledgments

This work was supported by the Natural Science Foundation of China (no. 51503110), the Program for Changjiang Scholars and Innovative Research Team in University (IRT_14R30), and the Program for Tanshan Scholar of Shandong Province, China.

References

[1] J. Cai, Q. Dang, C. Liu et al., "Preparation, characterization and antibacterial activity of *O*-acetyl-chitosan-*N*-2-hydroxypropyl trimethyl ammonium chloride," *International Journal of Biological Macromolecules*, vol. 80, pp. 8–15, 2015.

[2] T. Wang, Y. Zhou, W. Xie, L. Chen, H. Zheng, and L. Fan, "Preparation and anticoagulant activity of N-succinyl chitosan sulfates," *International Journal of Biological Macromolecules*, vol. 51, no. 5, pp. 808–814, 2012.

[3] T. Wang, X.-K. Zhu, X.-T. Xue, and D.-Y. Wu, "Hydrogel sheets of chitosan, honey and gelatin as burn wound dressings," *Carbohydrate Polymers*, vol. 88, no. 1, pp. 75–83, 2012.

[4] F. Croisier and C. Jérôme, "Chitosan-based biomaterials for tissue engineering," *European Polymer Journal*, vol. 49, no. 4, pp. 780–792, 2013.

[5] W. Paul and C. P. Sharma, "Chitosan and alginate wound dressings: a short review," *Trends in Biomaterials & Artificial Organs*, vol. 18, p. 18, 2004.

[6] R. Jayakumar, N. Nwe, S. Tokura, and H. Tamura, "Sulfated chitin and chitosan as novel biomaterials," *International Journal of Biological Macromolecules*, vol. 40, no. 3, pp. 175–181, 2007.

[7] R. Jayakumar, M. Prabaharan, R. L. Reis, and J. F. Mano, "Graft copolymerized chitosan—present status and applications," *Carbohydrate Polymers*, vol. 62, no. 2, pp. 142–158, 2005.

[8] J. H. Park, Y. W. Cho, H. Chung, I. C. Kwon, and S. Y. Jeong, "Synthesis and characterization of sugar-bearing chitosan derivatives: aqueous solubility and biodegradability," *Biomacromolecules*, vol. 4, no. 4, pp. 1087–1091, 2003.

[9] E. I. Rabea, E. T. Badawy, C. V. Stevens, G. Smagghe, and W. Steurbaut, "Chitosan as antimicrobial agent: applications and mode of action," *Biomacromolecules*, vol. 4, no. 6, pp. 1457–1465, 2003.

[10] R. A. A. Muzzarelli, "Biochemical significance of exogenous chitins and chitosans in animals and patients," *Carbohydrate Polymers*, vol. 20, no. 1, pp. 7–16, 1993.

[11] R. A. A. Muzzarelli, J. Boudrant, D. Meyer, N. Manno, M. DeMarchis, and M. G. Paoletti, "Current views on fungal chitin/chitosan, human chitinases, food preservation, glucans, pectins and inulin: a tribute to Henri Braconnot, precursor of the carbohydrate polymers science, on the chitin bicentennial," *Carbohydrate Polymers*, vol. 87, no. 2, pp. 995–1012, 2012.

[12] C. Chen, L. Liu, T. Huang, Q. Wang, and Y. Fang, "Bubble template fabrication of chitosan/poly(vinyl alcohol) sponges for wound dressing applications," *International Journal of Biological Macromolecules*, vol. 62, pp. 188–193, 2013.

[13] Y. Zhou, H. Yang, X. Liu, J. Mao, S. Gu, and W. Xu, "Potential of quaternization-functionalized chitosan fiber for wound dressing," *International Journal of Biological Macromolecules*, vol. 52, pp. 327–332, 2013.

[14] Z. Zhong, P. Li, R. Xing, and S. Liu, "Antimicrobial activity of hydroxylbenzenesulfonailides derivatives of chitosan, chitosan sulfates and carboxymethyl chitosan," *International Journal of Biological Macromolecules*, vol. 45, no. 2, pp. 163–168, 2009.

[15] M. W. Sabaa, N. A. Mohamed, R. R. Mohamed, N. M. Khalil, and S. M. Abd El Latif, "Synthesis, characterization and antimicrobial activity of poly (*N*-vinyl imidazole) grafted carboxymethyl chitosan," *Carbohydrate Polymers*, vol. 79, no. 4, pp. 998–1005, 2010.

[16] Y. Qin, R. Xing, S. Liu et al., "Synthesis and antifungal properties of (4-tolyloxy)-pyrimidyl-α-aminophosphonates chitosan derivatives," *International Journal of Biological Macromolecules*, vol. 63, pp. 83–91, 2014.

[17] T. Xu, M. Xin, M. Li, H. Huang, S. Zhou, and J. Liu, "Synthesis, characterization, and antibacterial activity of *N*,*O*-quaternary ammonium chitosan," *Carbohydrate Research*, vol. 346, no. 15, pp. 2445–2450, 2011.

[18] M. Lavertu, Z. Xia, A. N. Serreqi et al., "A validated ^{1}H NMR method for the determination of the degree of deacetylation of chitosan," *Journal of Pharmaceutical and Biomedical Analysis*, vol. 32, no. 6, pp. 1149–1158, 2003.

[19] J. Cai, Q. Dang, C. Liu et al., "Preparation and characterization of *N*-benzoyl-*O*-acetyl-chitosan," *International Journal of Biological Macromolecules*, vol. 77, pp. 52–58, 2015.

[20] G. Ma, D. Yang, Y. Zhou, M. Xiao, J. F. Kennedy, and J. Nie, "Preparation and characterization of water-soluble *N*-alkylated chitosan," *Carbohydrate Polymers*, vol. 74, no. 1, pp. 121–126, 2008.

[21] J. Wang and H. Wang, "Preparation of soluble p-aminobenzoyl chitosan ester by Schiff's base and antibacterial activity of the derivatives," *International Journal of Biological Macromolecules*, vol. 48, no. 3, pp. 523–529, 2011.

[22] Y. Feng and W. Xia, "Preparation, characterization and antibacterial activity of water-soluble *O*-fumaryl-chitosan," *Carbohydrate Polymers*, vol. 83, no. 3, pp. 1169–1173, 2011.

[23] G. Ma, D. Yang, J. F. Kennedy, and J. Nie, "Synthesize and characterization of organic-soluble acylated chitosan," *Carbohydrate Polymers*, vol. 75, no. 3, pp. 390–394, 2009.

[24] L. Sun, Y. Du, L. Fan, X. Chen, and J. Yang, "Preparation, characterization and antimicrobial activity of quaternized carboxymethyl chitosan and application as pulp-cap," *Polymer*, vol. 47, no. 6, pp. 1796–1804, 2006.

[25] D. S. Lee, J. Y. Woo, C. B. Ahn, and J. Y. Je, "Chitosan–hydroxycinnamic acid conjugates: preparation, antioxidant and antimicrobial activity," *Food Chemistry*, vol. 148, pp. 97–104, 2014.

[26] H. Tang, P. Zhang, T. L. Kieft et al., "Antibacterial action of a novel functionalized chitosan-arginine against Gram-negative bacteria," *Acta Biomaterialia*, vol. 6, no. 7, pp. 2562–2571, 2010.

[27] Q. L. Feng, J. Wu, G. Q. Chen, F. Z. Cui, T. N. Kim, and J. O. Kim, "A mechanistic study of the antibacterial effect of silver ions on *Escherichia coli* and *Staphylococcus aureus*," *Journal of Biomedical Materials Research*, vol. 52, no. 4, pp. 662–668, 2000.

[28] W. Sajomsang, S. Tantayanon, V. Tangpasuthadol, and W. H. Daly, "Quaternization of *N*-aryl chitosan derivatives: synthesis, characterization, and antibacterial activity," *Carbohydrate Research*, vol. 344, no. 18, pp. 2502–2511, 2009.

[29] K. K. Yang, M. Kong, Y. N. Wei et al., "Folate-modified–chitosan-coated liposomes for tumor-targeted drug delivery," *Journal of Materials Science*, vol. 48, no. 4, pp. 1717–1728, 2013.

[30] W. Sajomsang, P. Gonil, and S. Tantayanon, "Antibacterial activity of quaternary ammonium chitosan containing mono or disaccharide moieties: preparation and characterization," *International Journal of Biological Macromolecules*, vol. 44, no. 5, pp. 419–427, 2009.